Chemoselective hydrogenation of cinnamaldehyde at atmospheric pressure over combustion synthesized Pd catalysts

Dipak Das[a], Kamalesh Pal[a], Jordi Llorca[b], Montserrat Dominguez[b], Sara Colussi[c], Alessandro Trovarelli[c] and Arup Gayen[a,*]

[a] Department of Chemistry, Jadavpur University, Kolkata– 700032, India

[b]Institut de Tècniques Energètiques, Barcelona Research Center in Multiscale Science and Engineering, and Department of Chemical Engineering, Universitat Politècnica de Catalunya, 08019 Barcelona, Spain

[c]Dipartimento Politecnico, Università di Udine, 33100 Udine, Italy

---

[*]Corresponding author ; e-mail: agayenju@yahoo.com

Ph: +91-33-2457-2767 ; Fax: +91-33-2414-6223

Abstract

A series of Pd-supported metal oxides (Al_2O_3, Fe_2O_3 and CeO_2) have been prepared by a single step solution combustion synthesis (SCS). Their catalytic performance was evaluated for selective hydrogenation of cinnamaldehyde (CAL) to hydrocinnamaldehyde (HCAL) under atmospheric pressure of hydrogen at 100 °C. Among these materials, combustion synthesized Pd (2 at.%)/Al_2O_3 catalyst exhibits the highest CAL conversion (69 %) with complete HCAL selectivity. The analogous catalyst prepared by the incipient wetness impregnation (IWI) method shows an initially similar activity. XRD and HRTEM analyses of the as prepared SCS sample show fine dispersion of PdO over the γ-Al_2O_3 support. On ageing, a major portion of PdO is reduced to metallic Pd (Pd^{2+}:Pd^0=36:64 for the SCS catalyst and Pd^{2+}:Pd^0=26:74 for the IWI catalyst from XPS studies) suggesting comparatively more ionic character of palladium in the SCS catalyst. In the hydrogen atmosphere, without distinguishing the reductive pretreatment of catalyst and the beginning of hydrogenation subsequent to CAL addition, the Pd-species undergoes rearrangement to form a core-shell like structure of Pd (core)-PdO (periphery) covered with alumina layer, bringing in additional stability to the Pd-species in the SCS catalyst and making it highly recyclable. The analogous IWI catalyst, on the contrary, contains a mixed Pd-PdO ensemble that does not increase the stability causing continuous loss of activity in the consecutive cycles of hydrogenation.

Keywords: Palladium; Alumina; Atmospheric pressure hydrogenation; Cinnamaldehyde; Hydrocinnamaldehyde

1. Introduction

Research in heterogeneous catalysis is increasingly focused on the chemo- and regio-selective catalytic hydrogenation of α,β-unsaturated carbonyl compounds not only for the production of fine chemicals but also for scientific interest [1]. The chemoselective hydrogenation of such a carbonyl, namely cinnamaldehyde (C_6H_5–CH=CH–CH=O; CAL) to the semi hydrogenated products is the key step of the reaction. The hydrogenation at C=C site leads to the formation of hydrocinnamaldehyde (HCAL), while hydrogenation at C=O site produces cinnamyl alcohol (COL). Further hydrogenation of these two partially hydrogenated products produces hydrocinnamyl alcohol (HCOL).

The alcohols are industrially valuable products and intermediates for the synthesis of various fine chemicals. They are typically applied in perfumery and food industries [2-4], while in pharmaceutical industrial processes alcohol is used as an intermediate [3, 5]. Hydrogenation path yielding saturated carbonyls is a thermodynamically favorable process [6, 7]. HCAL has been reported to be an important intermediate in the preparation of pharmaceuticals used in the treatment of AIDS [8]. The selectivity and catalytic activity are influenced by several factors including reaction conditions and operation mode (gas or liquid phase hydrogenation), electronic and geometric structures of the metal catalysts, type of catalyst supports, catalyst preparation and activation procedures [9-13] and the polarity of solvent [14, 15].

Various attempts have been made to develop a suitable catalyst system for the selective (C=C vs. C=O) hydrogenation of CAL both in the gas-phase and in the liquid-phase [16-28]. Most of the studies use a high pressure of hydrogen and very few studies are available in the literature that have been carried out at atmospheric pressure. Despite several studies, CAL

hydrogenation with complete HCAL selectivity at atmospheric pressure remains a challenging issue in liquid phase hydrogenation.

The literature reports show that noble metal based catalysts are highly selective towards either COL or HCAL. In general, the Pd-based catalysts are more selective towards the C=C bond hydrogenation. Pt [16], Ru [17, 18], Au [19], Ir [20] and Ni-Co bimetallic [21] catalysts have been reported to be selective for the hydrogenation of C=O to unsaturated alcohol. On the other hand, Pd [12, 21-24], Ni [25], Rh [26], Pt [9], Pt-Au [9] are selective for the hydrogenation of C=C to form saturated aldehyde. Literature report also shows that smaller Pd particle is selective towards C=C hydrogenation, forming HCAL, while larger Pd particle is selective towards C=O hydrogenation, forming HCOL [27]. Espro et al. have also demonstrated the C=O bond selectivity of Pd-based catalysts in CAL hydrogenation under mild conditions [28].

The catalytic activity also depends on the acidity or the basicity and structural characteristics (particles size and porosity) of the support [29, 30]. Different types of supported palladium catalysts such as Pd/carbon [31, 32], Pd/SiO_2 [33], Pd/Al_2O_3 [34], Pd/TiO_2 [35], Pd/Fe_2O_3@C [36] have been reported to be efficient catalytic system for the hydrogenation of cinnamaldehyde. Graphene-supported Ni nanocatalyst shows selective hydrogenation towards C=C bond under atmospheric pressure [25]. Szumełda et al. have shown that carbon supported PdAu catalyst also shows selective hydrogenation activity under atmospheric pressure [37]. High surface area alumina with narrow pore size distribution acts as an effective support for catalytic reaction [34].

From the above literature survey, it would be very interesting to develop an active and selective supported metal catalyst system for the hydrogenation reaction under mild conditions. Over the last two-three decades, many researchers including us have shown the solution

combustion method to be a novel synthetic methodology to prepare metal/metal ion supported/doped oxide based materials that are reported to have promising activity behavior in various reactions of technological importance [38-41]. Motivated further by these findings and the objective of this present work, we have studied the hydrogenation of cinnamaldehyde in liquid-phase on CeO_2, Fe_2O_3 and Al_2O_3 supported Pd catalysts prepared by a facile solution combustion method using molecular hydrogen at atmospheric pressure in different solvents. We show that highly dispersed palladium on alumina exhibits a good conversion with complete HCAL selectivity towards CAL hydrogenation in 1,4-dioxane at 100 °C and atmospheric pressure.

2. Experimental

2.1. Preparation of materials

The Pd-supported oxide (Al_2O_3, CeO_2 and Fe_2O_3) catalysts were prepared via a facile solution combustion method. As an example, Pd (2 at.%)/Al_2O_3 is prepared through combustion of a redox mixture of $Al(NO_3)_3.9H_2O$ and 1% $PdCl_2$ solution with oxalyl dihydrazide (ODH, $C_2H_6N_4O_2$), taken in a stoichiometric ratio of 1.96:0.04:2.94, at the ignition temperature of ~450 °C. Typically, 10 g of $Al(NO_3)_3.9H_2O$ (Merck India, 99%), 9.6 mL solution of 1% $PdCl_2$ (Arora Matthey Ltd., 40% Pd) and 4.73 g of ODH are taken in a borosilicate dish and homogenized with ~30 mL of double distilled water by gentle heating. Subsequently, the dish is introduced to a muffle furnace maintained at ~450 °C for combustion. After complete dehydration, the surface of the reaction crude gets ignited and burns with a flame forming a voluminous solid product within a minute. The ceria and ferric oxide supported Pd samples were prepared similarly using

$(NH_4)_2Ce(NO_3)_6$ (Merck, GR, 99%) and $Fe(NO_3)_3.9H_2O$ (Merck India, 99 %) as the precursor salts. The materials studied for CAL hydrogenation are listed in **Table 1**.

Table 1. Nominal composition, name, Pd-loading (nominal), surface area and hydrogenation[a] behavior of different palladium supported catalysts at 100 °C

Nominal composition	**Name**	**Pd (wt.%)**	**SA ($m^2 g^{-1}$)**	**Conv[b] (%)**	**Sel[c] (%)**
Al_2O_3	–	–	42	–	–
Pd (2 at.%)/CeO_2	Pd2Ce	1.2	15	24	83
Pd (1.5 at.%)/Fe_2O_3	Pd1.5Fe	2.0	24	59	93
Pd (1 at.%)/Al_2O_3	Pd1Al	2.0	49	43	100
Pd (2 at.%)/Al_2O_3	Pd2Al	4.0	51	69	100
Pd (3 at.%)/Al_2O_3	Pd3Al	6.0	52	71	97
Pd (2 at.%)/Al_2O_3 IWI	Pd2AlIWI	4.0	51	67	100

[a] Reaction condition: 0.1 g catalyst, 1 mL cinnamaldehyde, 40 mL 1,4-dioxane, 100 °C, 3 h, H_2 pressure = 1 atm; [b] Conv = CAL conversion; [c] Sel = HCAL selectivity.

For better comparison of the hydrogenation activity, we have also prepared the Pd(2 at. %)/Al_2O_3 catalyst by the incipient wetness impregnation (IWI) method. In this method, Al_2O_3 support made via solution combustion was impregnated with requisite amount (for 2 at. % Pd-loading) of aqueous $Pd(NO_3)_2$ solution corresponding to the support pore volume. The Pd-impregnated sample was then dried overnight at 100 °C, crushed and calcined at 450 °C for 3 h in air to prepare the catalyst (named as Pd2AlIWI ; see **Table 1**).

2.2. Characterization of materials

The powder X-ray diffraction (XRD) data were collected using Cu Kα radiation (λ= 1.5418 Å) on a Bruker D8 Advance X-ray diffractometer operated at 40 kV and 40 mA. The

XRD patterns were recorded in the 2θ range of 20–80° using Lynxeye detector (1D mode) with a dwell time of 0.4 s per step and analyzed by ICDD (International Centre for Diffraction Data) database for phase identification. Average particle sizes were calculated from the broadening of the most intense diffraction peaks using the Scherrer's equation.

The BET specific surface areas were measured in a TriStar3000 surface area analyzer (Micromeritics). Before each measurement, the samples were degassed at 150 °C in vacuum for 90 min, cooled to room temperature and immediately mounted in the sample port for analysis.

The microstructure of the samples was analyzed by High Resolution Transmission Electron Microscopy (HRTEM) performed in a JEOL 2010F instrument equipped with a field emission electron source at an accelerating voltage of 200 kV. The resolution between lines was 0.14 nm and the point-to-point resolution was 0.19 nm. The magnification was calibrated against a Si standard. We did not observe any damage of the samples under prolonged electron beam exposure. The samples were dispersed ultrasonically in ethanol to form a suspension and a drop of it was placed on a holey-carbon coated grid. All the images correspond to raw data.

X-ray photoelectron spectroscopy (XPS) study was carried out on a SPECS system equipped with an Al anode XR50 source operating at 150 mW and a Phoibos 150 MCD-9 detector. The sample powders were pressed to self-consistent disks and an area of 2 mm × 2 mm was analyzed. The analysis chamber was maintained always below 10^{-7} Pa. The pass energy of the hemispherical analyzer was set at 25 eV and the energy step was set at 0.1 eV. A SPECS Flood Gun FG 15/40 took care of charge stabilization. At first the survey spectrum followed by XP spectrum of C 1s, O 1s, Al 2p and Pd 3d and C 1s again were recorded to check for charge stability and the absence of sample degradation during the analyses. The data were processed with the CasaXPS program (Casa Software Ltd., UK). The binding energy (BE) values were

calculated with respect to the C 1s peak at 284.8 eV. Atomic fractions (%) were calculated using peak areas normalized on the basis of acquisition parameters after background subtraction, experimental sensitivity factors and the transmission factors provided by the manufacturer.

The redox behavior of the materials was assessed by Temperature Programmed Reduction (TPR) experiments using a Micromeritics Autochem apparatus equipped with a TCD detector. In a typical experiment, the sample was pre-treated in air at 450 °C for 1 h to remove adsorbed species, then cooled down to -80 °C under liquid nitrogen flush. The flowing gas was then switched to a mixture of 5 vol. % H_2 in N_2 and the temperature was ramped to 500 °C at 10 °C min^{-1} while recording hydrogen consumption.

Pulse CO chemisorption experiments were carried out in the same Micromeritics Autochem apparatus. Prior to pulse experiments, the samples were treated at 100 °C for 1 h in a mixture containing 5 vol % H_2 in N_2 (similar to the pretreatment before reaction experiments). After cooling down to room temperature, the samples were exposed to pulses of 5 vol % CO in He. The pulses were repeated until no CO chemisorption took place.

2.3. Test of hydrogenation activity

In a typical experiment, 40 mL of solvent was taken in a two necked 100 mL round bottom flask to which 0.1 g of catalyst material was added. Nitrogen was bubbled through the liquid-phase under stirring (rpm= 700) condition for ~30 min in order to remove traces of dissolved oxygen from the medium. The catalyst was then reduced under flowing hydrogen (10 mL min^{-1}) at 100 °C for 45 min. This was followed by introduction of 1 mL of cinnamaldehyde to commence the hydrogenation reaction. Hydrogen gas was continuously bubbled (10 mL min^{-1}) through the liquid phase under stirring condition throughout the progress of the reaction.

The composition of the reaction mixture was analyzed immediately after centrifugation (REMI RM-12CDX; rpm= 5000) of the reaction aliquot (0.5 mL) using a Nucon 5765 (New Delhi, India) gas chromatograph fitted with a fused silica capillary column (EC5) of dimension 10 m × 0.25 mm × 0.25 μm (length × diameter × film thickness) from Alltech and equipped with a FID detector. The temperatures of the injector and the detector were maintained respectively at 220 °C and 240 °C. The initial and the final column temperatures were 110 °C and 150 °C, respectively at a rate of 80 °C min^{-1}.

The CAL conversion (Conv) and HCAL selectivity (Sel) have been defined by the following equations:

$$Conv = \frac{(mol_{CAL})_{initial} - (mol_{CAL})_{final}}{(mol_{CAL})_{initial}} \times 100 \quad (4)$$

$$Sel = \frac{mol_{HCAL}}{mol_{HCAL} + mol_{HCOL}} \times 100 \quad (5)$$

Where mol_{CAL}, mol_{HCAL} and mol_{HCOL} are the moles of CAL, HCAL and HCOL, respectively. No COL was ever detected in our analysis.

3. Results and Discussion

3.1. BET studies

The specific surface area of the alumina based samples is similar and fall in the range 42-52 m^2 g^{-1} (see **Table 1**). The presence of Pd over alumina increases the SA in general irrespective of the preparation route, SCS or IWI. The CeO_2 or Fe_2O_3 based oxides exhibit a lower surface area.

3.2. Screening of materials

Use of a small amount of catalyst in its powder (finely divided) form, maintaining a sufficiently high rpm during hydrogenation and allowing a considerable reaction time in all the catalytic runs of this study eliminated the involvement of any mass transfer influence in the reaction as reported by us in an earlier study [42]. Initial activity screening over the materials showed the Pd-loaded alumina samples to show complete HCAL selectivity (see **Table 1**) up to 2 at. % Pd (or 4 wt.% Pd ; nominal). The Pd2Ce sample showed the lowest hydrogenation activity and selectivity towards the desired product. Despite its lower surface area, the 1.5 at.% Pd-loaded Fe_2O_3 sample, Pd1.5Fe, containing about 2 wt. % Pd shows a higher conversion than its Al_2O_3 analogue, but it suffers from a lower selectivity (see **Table 1**). We thus chose Pd-loaded alumina samples for further investigation.

3.3. XRD studies

The powder XRD patterns of as prepared Al_2O_3 and all the Pd loaded Al_2O_3 samples are shown in **Figure 1**. The diffraction peaks correspond to the gamma phase of alumina (JCPDS PDF # 770396) and palladium oxide (JCPDS PDF # 411107). Evidence of metallic palladium formation together with PdO in the as prepared samples is not clear due to broad nature of the diffraction peaks and to the overlapping of Pd^0 related diffraction peaks with those of the alumina peaks. The crystallite size is about 7 nm for alumina (from the broadening of (440) peak), while the size of PdO falls in the range 10-13 nm (from (101) peak broadening) depending on Pd-loading for the combustion made samples. On the other hand, the PdO crystallites in the IWI catalyst are comparatively smaller in size (~6 nm).

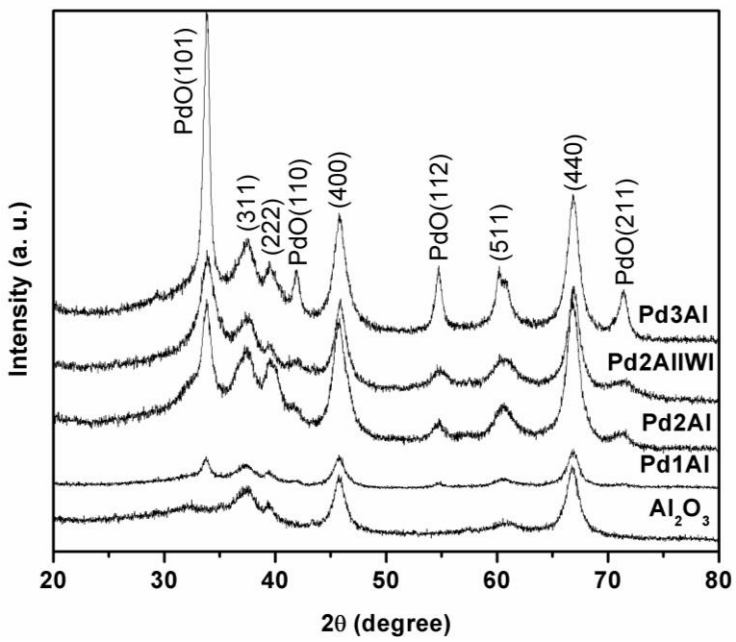

Figure 1. Powder XRD patterns of as prepared Al_2O_3 and various Pd/Al_2O_3 catalysts via SCS and IWI methods

3.4. Effects of Pd-loading, reaction time and temperature

The Pd loading over Al_2O_3 greatly influences the catalytic performance of cinnamaldehyde hydrogenation (see **Table 1**). A lower Pd loading of 1 at. % over Al_2O_3 shows lower conversion (43%) of CAL with complete selectivity of HCAL. With the increase of Pd loading to 2 at. % the conversion increases to 69% with 100% selectivity of HCAL. Further increase of Pd loading to 3 at. % increases the conversion only marginally (from 69% to 71%), but the selectivity decreases from 100% to 97%. Interestingly, 2 at. % Pd loaded over Al_2O_3 by IWI (Pd2AlIWI) method also gives a hydrogenation activity similar to the SCS catalyst, showing 67% conversion with 100% selectivity in 3 h at 100 °C.

The time dependent conversion of CAL over Pd2Al, as well as HCAL selectivity, is shown in **Figure 2(a)**. As can be observed, 17% conversion takes place in first 1 h. After this time, the conversion increases sharply up to 3 h and reaches 70% with 100% selectivity of

HCAL. Afterwards, the conversion increases slowly (only 4 % conversion takes place in next 1 h) and is associated with a decrease of selectivity from 100 % to 98 %. During the course of reaction, we did not observe the formation of cinnamylalcohol. At the end of 5 h, 76 % conversion of the CAL occurs with 92 % HCAL selectivity.

The influence of temperature on the hydrogenation of CAL over Pd2Al was studied by varying the temperature from 30 °C to 110 °C and keeping all the other parameters constant (**Figure 2(b)**). No hydrogenation seems to occur at room temperature. When the reaction temperature is increased to 60 °C, the conversion reaches 23 %, being 61 % at 80 °C and 69 % at 100 °C. A further temperature increase to 110 °C does not improve the overall activity. However, the selectivity of HCAL is 100 %.

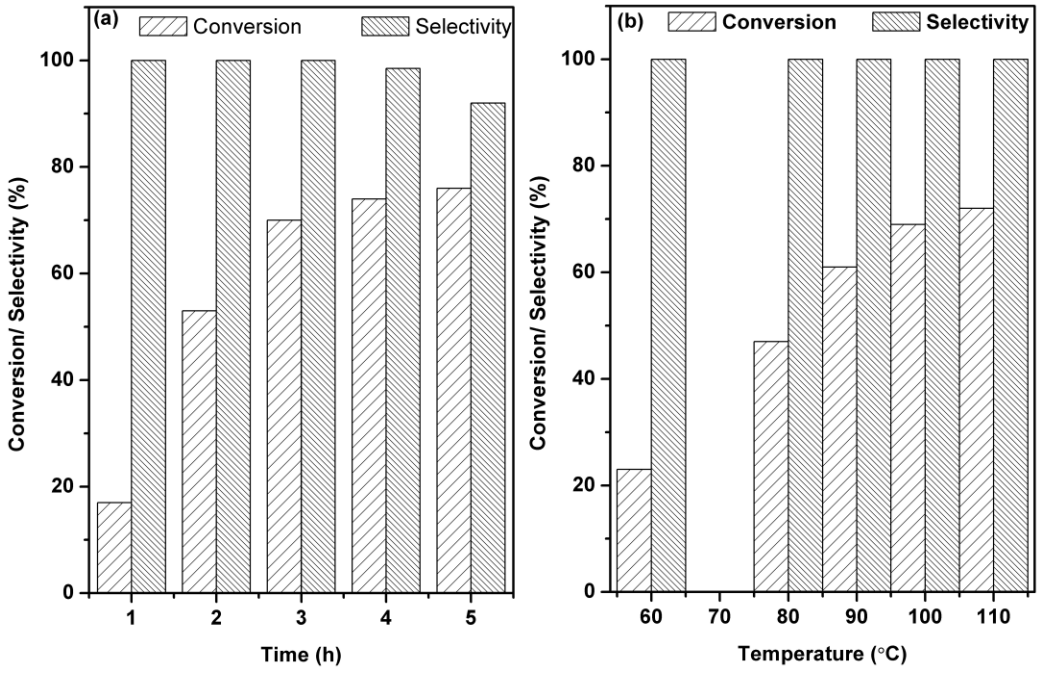

Figure 2. Cinnamaldehyde hydrogenation activity of Pd2Al as a function of (a) reaction time at 100 °C and (b) temperature after 3 h of reaction. Reaction condition: 0.1 g catalyst, 1 mL cinnamaldehyde, 40 mL 1,4-dioxane

3.5. Effect of solvent

Figure 3(a) shows the hydrogenation activity of Pd2Al in different solvents. In agreement with the literature, the polar protic solvent hexanol exhibits the highest conversion (92%) with a lower HCAL selectivity (79%) than that obtained using the polar solvent DMF and the non-ploar solvent 1,4-dioxane [11]. The conversion of CAL in DMF is the lowest (58%), which might be attributed to the fact that the reactants are less soluble in it [43]. Hydrogenation in 1,4-dioxane takes place with a moderate conversion but with complete selectivity of HCAL. To avoid the transfer hydrogenation of CAL in the presence of a hydrogen donating solvent (hexanol, a polar protic solvent, in our case), we used 1,4-dioxane as a solvent because it is inert during the hydrogenation reaction and it also improves HCAL selectivity [9, 12, 44]. A sufficiently high rpm of 700 and continuous flow of pure hydrogen at 10 mL min^{-1} were used to ensure that the hydrogenation reaction is not limited by hydrogen solubility in the solvents.

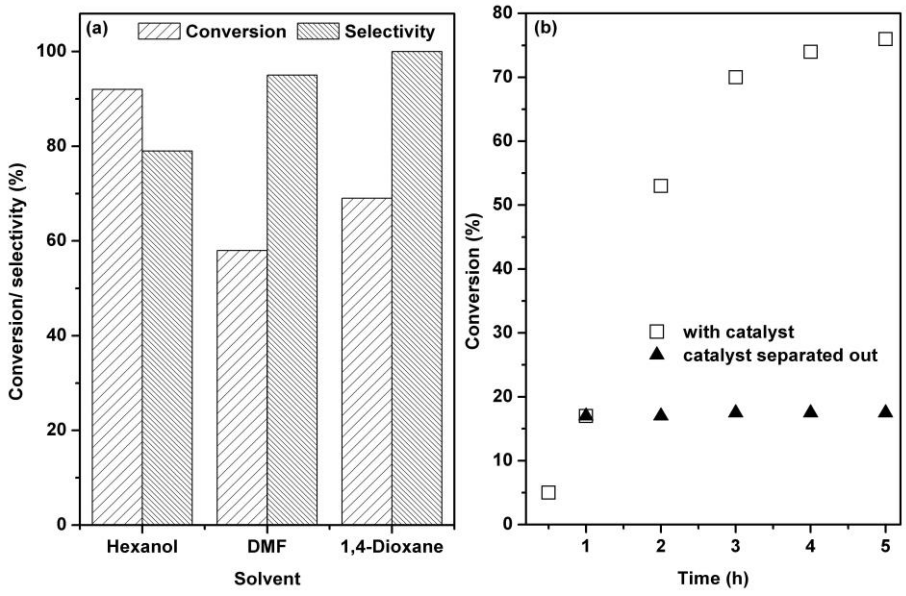

Figure 3. (a) Effect of solvent on CAL hydrogenation (after 3 h) over Pd2Al and (b) activity data of Sheldon's hot filtration test. Reaction condition: 0.1 g catalyst, 1 mL CAL, 40 mL 1,4-dioxane, 100 °C

3.6. Hot filtration test

To establish the heterogeneous nature of the Pd2Al catalyst for the hydrogenation of CAL, we have performed the conventional hot filtration test of Sheldon [45]. The hot reaction mixture was separated from the catalyst immediately after 1 h of reaction (when 17 % conversion was reached) by filtering through a Gooch (G4) at the reaction temperature (100 °C) in order to avoid re-adsorption of leached metals, if any, onto the catalyst surface. The filtrate was collected into another preheated round bottom flask maintained at the reaction temperature and the activity behavior of the filtrate was studied for further 4 h (see **Figure 3(b)**). The gas chromatographic analysis of the isolated solution did not exhibit any further reactivity up to 5 h of reaction. This result establishes a truly heterogeneous nature of the activity onto the facile combustion synthesized catalyst.

3.7. Catalyst recyclability

For a better comparison, we have studied also the recycling ability of the Pd2Al and Pd2AlIWI catalysts. After each cycle of reaction, the catalyst was separated by centrifugation and washed thoroughly with ethanol and dried in an oven at 100 °C before use in the next cycle. Initially, both the fresh SCS and IWI catalysts show similar activity pattern (see **Figure 4**). Afterwards, the conversion and selectivity of the IWI catalyst decreases continuously up to the third cycle. Though the conversion exhibited by the IWI catalyst remains the same in the fourth cycle, the HCAL selectivity decreases slightly. The SCS catalyst, on the contrary, experiences only a minor decrease in conversion and selectivity after the fourth cycle of test exhibiting 66 % CAL conversion with 99 % HCAL selectivity. The recycling test thus indicates a higher stability

of the SCS catalyst with respect to the analogous IWI catalyst under the reaction conditions of this study.

The differences in the hydrogenation activities of the SCS and analogous IWI catalysts might be attributed to the differences in surface characteristics and microstructure of the materials. Detailed XRD phase analysis of aged catalysts (sample collected after four consecutive cycles of hydrogenation), XPS surface analysis and HRTEM microstructural analysis were thus carried out, together with H_2-TPR and CO chemisorptions experiments.

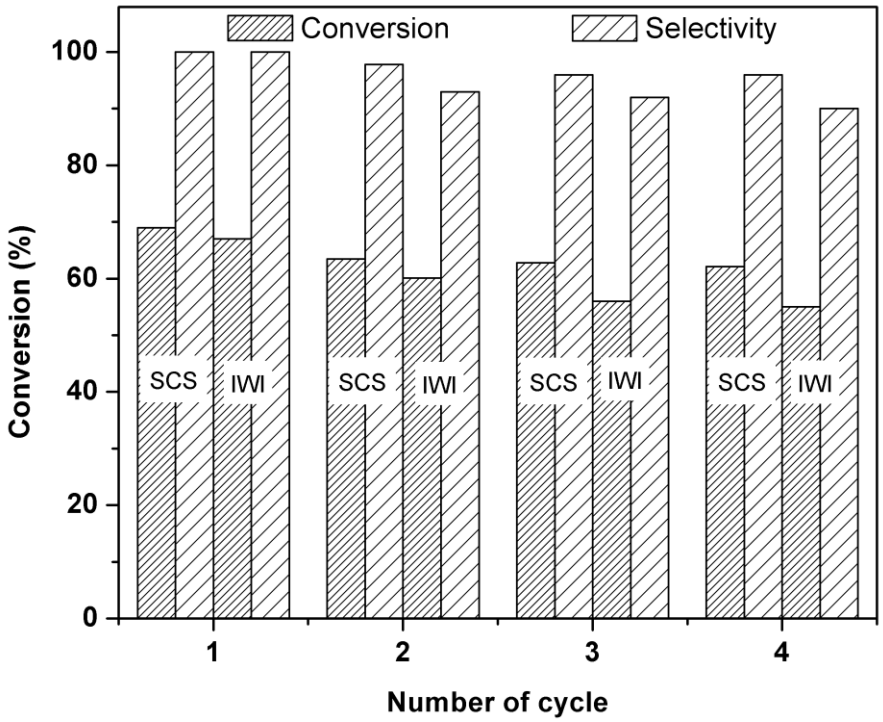

Figure 4. Effect of cycling on cinnamaldehyde hydrogenation over Pd2Al and Pd2AlIWI. Reaction condition: Pd2Al = 0.1 g, cinnamaldehyde = 1 mL, 1,4-dioxane = 40 mL, 100 °C, 3 h

3.8. TPR experiments

Figure S1 shows the TPR profiles recorded for Pd2Al and Pd2Al IWI. The samples have been pre-treated in air in order to remove all carbon containing species that may arise during the

synthesis. The main thing to observe is that on Pd2Al the reduction starts at a lower temperature (-15 °C with respect to 0 °C for 2PdAlIWI), and the hydrogen consumption peak is clearly divided into more than one feature, indicating the coexistence of different PdO species with different interaction with the support [46]. Moreover, the negative peak observed at about 55 °C and corresponding to the decomposition of Pd hydrides is much more pronounced for Pd2Al; this might point to a higher affinity for hydrogen of Pd contained in the SCS sample with respect to the IWI sample, in accordance to the higher reducibility of Pd2Al at a lower temperature.

3.9. XRD studies of aged catalysts

From the TPR studies it is obvious that all the PdO is reduced to Pd metal (JCPDS PDF # 461043; see **Figure S2**) in the reducing atmosphere of pretreatment which is maintained also during the actual hydrogenation reaction. The crystallite size of the oxide support and the dispersed Pd-phase remains essentially the same on the combustion synthesized catalyst Pd2Al upon ageing. On the contrary, the PdO crystallites in the IWI catalyst grow a little (from ~6 nm to ~8 nm) on the aged catalyst.

3.10. XPS studies

Figure S3 shows the Pd 3d XP spectra of the Pd2Al (combustion made and impregnated) catalysts in their as prepared and aged forms. The data are tabulated in **Table 2**, which also includes the data for Pd3Al (spectra not included here).

The only species present in the samples are Pd metal and Pd^{2+} [35]. Initially, the sample Pd2Al contains only oxidized Pd; whereas the sample Pd3Al contains both oxidized and metallic Pd, the former being the major species on the surface. The binding energy values of oxidized Pd

species indicates formation of PdO during the SCS preparation, which turns out to be the only Pd-species at a lower loading of 2 at. %. But for the higher Pd-loaded sample, Pd3Al, small Pd metal nanoparticles are formed together with PdO. Unlike the as synthesized combustion made Pd2Al, the analogous impregnated sample Pd2AlIWI contains both reduced and oxidized Pd. About the aged samples, it is clear in all cases that in the course of prolonged (up to four consecutive cycles) presence of the catalyst in the hydrogen atmosphere maintained in the reaction medium, Pd suffers strong reduction, as it is mainly metallic in both Pd2Alaged and Pd2AlIWIaged samples (64.2 and 73.7 %, respectively), but some oxidized Pd species also remain, mainly in the SCS sample. The reductive pretreatment of the catalyst in the liquid phase before starting the hydrogenation reaction is expected to produce essentially metallic palladium species in line with the TPR findings. Existence of a portion of oxidized Pd-species even in the aged samples appears to be due to the oxidation of metallic Pd on exposure to air during sample transfer to the XPS chamber.

Table 2. The binding energies and the surface atomic concentrations of the reduced and oxidized Pd and Pd/Al ratios of the various catalysts

Sample	**Name**	**Position (eV)**	**% At Pd^0**	**% At Pd^{2+}**	**Pd/Al**
Pd2Al	Pd $3d_{5/2}$ (Pd^0)	–	0	100	0.012
	Pd $3d_{5/2}$ (Pd^{2+})	336.3			
	Al $2p_{3/2}$	74.3			
Pd3Al	Pd $3d_{5/2}$ (Pd^0)	334.6	29	71	0.015
	Pd $3d_{5/2}$ (Pd^{2+})	336.2			
	Al $2p_{3/2}$	74.3			
Pd2Alaged	Pd $3d_{5/2}$ (Pd^0)	335.1	64	36	0.010
	Pd $3d_{5/2}$ (Pd^{2+})	336.8			

	Al $2p_{3/2}$	74.3			
Pd2AlIWI	Pd $3d_{5/2}$ (Pd^0) Pd $3d_{5/2}$ (Pd^{2+}) Al $2p_{3/2}$	334.8 336.5 74.3	17	83	0.030
Pd2AlIWIaged	Pd $3d_{5/2}$ (Pd^0) Pd $3d_{5/2}$ (Pd^{2+}) Al $2p_{3/2}$	335.1 337.4 74.3	74	26	0.028

Aluminium is found to maintain its robust oxidation state of 3+ in the catalyst (the 2p peak (spectra not included here) centered at 74.3 eV corresponds to Al^{3+}) [47] that does not change due to ageing.

Concerning the surface atomic ratios, the sample Pd2Al exhibits a Pd/Al ratio of 0.012, which is less than the expected value of 0.020 in $Pd_{0.04}Al_{1.96}O_3$. The same applies to sample Pd3Al, which exhibits an atomic Pd/Al ratio of 0.015, which is less than the nominal value of 0.031 in $Pd_{0.06}Al_{1.94}O_3$. The sample Pd2AlIWI exhibits a much higher Pd/Al atomic ratio, 0.030 (the theoretically expected value is 0.020). This could be interpreted in terms of Pd deposition as well-dispersed nanoparticles over alumina in the IWI sample and essentially due to Pd encapsulation by the alumina support in the SCS samples, that is, all the Pd would be at the surface in the IWI sample whereas Pd would be somehow covered (not at the surface always) in the SCS samples. Presence of a portion of Pd within the bulk structure is yet another possibility that contributes to the lower surface Pd-concentration. The aged samples exhibit slightly lower Pd/Al atomic ratios with respect to the fresh samples both for Pd2Al and Pd2AlIWI, which means that a slight sintering of Pd occurs when exposed to hydrogen environment i.e., during reductive pretreatment and in the course of reaction.

3.11. TEM studies

The Pd2Al catalyst contains nanoparticles, mostly in the range 8-20 nm in diameter, well dispersed over the alumina support (**Figure 5(a)**). Remarkably, the nanoparticles are partially embedded into the alumina support. This explains why the Pd/Al ratio determined by XPS is low. A detailed lattice fringe analysis performed over various particles reveals that the nanoparticles are PdO. As an example, **Figure 5(b)** shows the HRTEM image of a nanoparticle measuring about 10 nm. The spacing measured in the Fourier Transform image (FT) at 2.6 Å corresponds to the (101) crystallographic plane of PdO. The existence of only PdO is fully in accordance to XPS results.

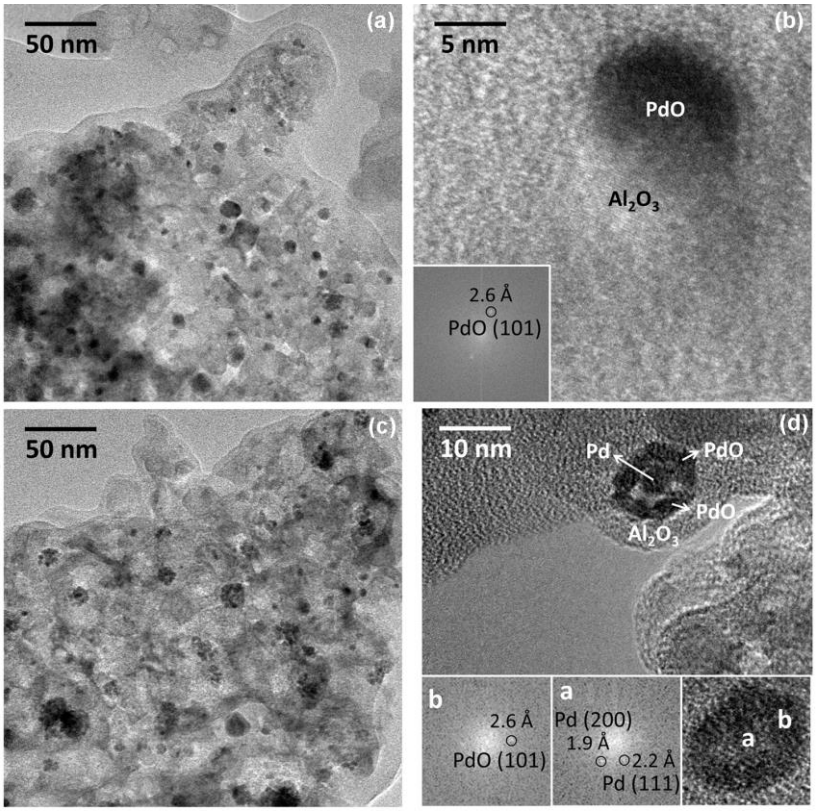

Figure 5. TEM images of (a, b) Pd2Al and (c, d) Pd2Alaged.

The Pd3Al sample is very similar to the Pd2Al sample. Well-dispersed nanoparticles mostly in the range 8-20 nm over alumina are evident in the TEM images (not included here). Again, an alumina shell is observed covering the catalyst particles, which explains the low Pd/Al atomic ratio measured by XPS.

The aged sample Pd2Alaged shows a distinct morphology when compared to the fresh Pd2Al catalyst (**Figure 5(c)**). The PdO particles mostly break apart and originate mixed particles between PdO and metallic Pd. This is nicely seen in the HRTEM image shown in **Figure 5(d)**. The FT image recorded inside the particle (area labeled "a") shows spots at 2.6 Å of PdO, but the FT images recorded in the peripheral particles of the agglomerate clearly show lattice fringes at 2.2 and 1.9 Å, which correspond to metallic Pd. Therefore, the PdO nanoparticles partially reduce in the hydrogen atmosphere and originate an agglomerate structure of Pd-PdO, possibly as Pd(core)-PdO(periphery). On the other hand, the alumina layer covering the Pd-containing nanoparticles is clearly seen in **Figure 5(d)**. The alumina covered PdO particles are expected to be reduced latter than the dispersed PdO particles in the liquid phase. We may attribute the Pd-PdO agglomerate formation to the different extents of reduction of the two types of Pd-species and vigorous stirring of the reaction mixture.

The catalyst prepared by conventional incipient wetness impregnation (Pd2AlIWI) does not contain an alumina layer over the Pd-containing nanoparticles. A general view is shown in **Figure S4(a)**. The sample is comprised mostly by nanoparticles of 4-15 nm in diameter. The smaller size of the nanoparticles and the absence of the alumina layer explain perfectly why this sample has a higher Pd/Al atomic ratio measured by XPS than the equivalent sample prepared by solution combustion method (Pd2Al). A detailed HRTEM image is shown in **Figure S4(b)**. The small nanoparticles measuring about 4 nm in diameter exhibit lattice fringes at 2.2 and 1.9 Å,

which correspond to the (111) and (200) crystallographic planes of metallic Pd, respectively. The larger particles exhibit lattice fringes corresponding to PdO. The sample contains a mixture of PdO and Pd, being the smaller particles metallic Pd and the larger ones, PdO.

After reaction, the impregnated catalyst Pd2AlIWIaged has suffered a similar transformation than the Pd2Alaged sample and the PdO particles have broken apart and partially reduced. This is clear from **Figures S4(c)** and **S4(d)**. A careful analysis of the HRTEM image shown in **Figure S4(d)** reveals the presence of a mixed Pd-PdO particle. It appears that the particle was initially PdO, and that in the hydrogen environment underwent partial reduction to form a mixed Pd-PdO ensemble. This reduction is consistent with the XPS results, which showed an increase of metallic Pd with respect to oxidized Pd in the aged sample with respect to the fresh one.

3.12. CO chemisorptions studies

We have carried out the Pd-dispersion analysis of only the most active Pd2Al and its impregnated analogue Pd2AlIWI sample. The Pd-dispersion is found to be 3.3 % for the former catalyst and 5.0 % for the latter catalyst. The metallic surface areas are 0.6 m^2 g^{-1} and 0.9 m^2 g^{-1}, respectively for Pd2Al and Pd2AlIWI. The values are both very low, but it is understandable keeping in mind the conditions of synthesis for Pd2Al and the fact that for Pd2AlIWI the palladium is impregnated on a relatively low surface area support.

It is known from the literature that the Pd:CO stoichiometry can vary from 1 to 2 depending on the Pd particle size. The authors have not included this effect at all. **"**Concerning binding energy values, of course we are aware of the particle size effect but, in our case, we have

used the technique for surface atomic composition and we have not intended to use BEs to discuss about particle size."

3.13. Structure-activity correlation

The bulk phase analyses have revealed fine dispersion of PdO over the alumina support in both Pd2Al and Pd2AlIWI and presence of metallic Pd could not be ascertained due to overlap of its diffraction peaks with the Al_2O_3 peaks. The way of preparation of the analogous IWI catalyst though suggests presence of only highly dispersed PdO on the surface, it contains a minor portion of metallic Pd even in the as prepared catalyst. The findings of TEM and XPS studies support this, both of which point to the existence of palladium oxide and metallic palladium (absent in fresh Pd2Al) species on the surface of the SCS and IWI catalysts. The major change in surface composition of Pd-species after exposing the catalyst to hydrogen atmosphere is the increase of metallic Pd component. Since the samples were exposed to air during transfer to the XPS chamber, it may be possible that the metallic palladium is reoxidized. The surface areas are very similar for these two types (SCS and IWI) of materials. So, this can't explain the hydrogenation behavior exhibited by them. The recycling tests have indicated little but higher stability for the SCS catalyst and absence of leaching. The small deactivation recorded for various cycles may be due to some blockage of the catalyst surface by organic moiety. The microstructural findings of the fresh SCS catalyst have suggested the formation of embedded Pd-containing nanoparticles in the catalyst (that results in the lower Pd/Al atomic ratio) in contrary to highly dispersed palladium in the IWI catalyst (that is consistent with its higher Pd/Al atomic ratio). Simultaneously, the detailed HRTEM analysis of Pd2Alaged sample has indicated that there occurs partial reduction of the PdO nanoparticles in the solvent medium under hydrogen

atmosphere to originate a core-shell like structure of Pd (core)-PdO (periphery) covered with alumina layer. This microstructural transformation brings in additional stability to the Pd-species dispersed over alumina in the combustion synthesized catalyst. The scenario is completely different in the IWI catalyst prepared via multistep incipient wetness impregnation where there is formation of a mixed Pd-PdO ensemble due to the partial reduction of PdO nanoparticles that does not contribute further stability to the dispersed palladium surface species. This is reflected in the recycling behavior of the catalysts, Pd2Al showing better activity behavior than the Pd2AlIWI catalyst. This suggests SCS as a superior method to IWI for the preparation of Pd/Al_2O_3 catalyst for cinnamaldehyde hydrogenation.

The results of CO chemisorption measurements are in line with what is expected from the above findings; the IWI catalyst contains more exposed Pd while the SCS catalyst has a lower Pd-dispersion owing to its possible presence in a core-shell like structure (originated on hydrogen treatment). Despite a lower Pd-dispersion, the formation of a stable Pd (core)-PdO (periphery) structure covered with alumina layer in the combustion made catalyst contributes to its higher hydrogenation activity than the impregnated catalyst.

In general, metallic palladium interacts with the alkene moiety (C=C) more strongly than the carbonyl group (C=O) of CAL and yields HCAL. In our case unsaturated COL was not formed in detectable amount, HCAL was formed as the exclusive product. When more time was allowed for the hydrogenation, this HCAL was eventually converted to HCOL. The reduced palladium species (Pd^0) seems to be stabilized more in presence of the nonreducible support Al_2O_3 under reducing pretreatment/ reaction atmosphere. This metallic Pd species can polarize the C=C bond in an effective manner compared to the oxidized PdO species. We thus observed complete selectivity for HCAL over the Pd2Al catalyst. The presence of oxidized palladium

species (PdO), on the other hand, polarize the C=O moiety directing the reaction pathway through the formation of COL causing a lower HCAL selectivity. In the presence of a reducible support like CeO_2, complete reduction of PdO may not be possible and this can possibly explain the lowest activity behavior recorded for the ceria based materials. This is also true for the Pd/Fe_2O_3 catalyst and hence it did not show complete HCAL selectivity despite its good conversion behavior.

3.14. Comparison with other Pd-based catalytic systems

As mentioned earlier most of the studies on cinnamaldehyde hydrogenation use a high pressure of hydrogen and only a few studies are carried out at atmospheric pressure of hydrogen. Moreover, there are differences in other experimental parameters that make it difficult to compare directly these systems. Even so, in **Table 3** we try to make a comparison of the most relevant systems in regard to selective hydrogenation of C=C bond. The table also includes the activity data in mole of HCAL formed per gram of Pd (considering total Pd in the sample) per hour ($mol_{HCAL}\ g_{Pd}^{-1}\ h^{-1}$).

Table 3. Comparison of cinnamaldehyde hydrogenation behavior of the combustion synthesized Pd2Al with some of the Pd-based materials reported in the literature

Catalyst	**Solvent**	**Time (h)**	**P (bar)**	**T (°C)**	**Conv (%)**	**Sel* (%)**	**Activity ($mol_{HCAL}\ g_{Pd}^{-1}\ h^{-1}$)**	**Reference**
Pd (1.9 wt.%)/ γ-Al_2O_3	Decalin	3	20	100	99	94	3.73	[21]

5 wt.% Pd/Al_2O_3 (Aldrich)	Decalin	3	20	100	98	90	3.53	[21]
5 wt.% Pd/Al_2O_3 (Aldrich)	Ethanol	1	40	50	40	65	-	[22]
Pd/Al_2O_3 (thiol coated)	Ethanol	1	40	50	40	88	-	[22]
AuPd-OMC	2-propanol	11	1	40	97	88	1.47	[32]
Pd/ZIF	2-propanol	6	20	40	100	90	0.60	[11]
1.5 wt.% Pd-CNT/AC	1,4-dioxane	2	15	70	87	82	1.80	[12]
5 wt.% Pd/CNF	1,4-dioxane	30	1	80	100	98	2.47	[23]
Pd-Au/C	Toluene	1	1	22	100	65	-	[37]
5 wt.% Pd/Al_2O_3 (Aldrich)	1,4-dioxane	50	1	80	40	40	0.24	[23]
Pd (4 wt.%)/Al_2O_3	1,4-dioxane				69	100	0.45	
	DMF	3	1	100	58	95	0.36	This work
	Hexanol				92	79	0.47	

* Selectivity of HCAL

Galletti et al. have studied the CAL hydrogenation over Pd on γ-Al_2O_3, prepared by a microwave-assisted solvothermal synthesis using PVP as the capping agent. They have reported 98.8 % conversion with 93.8 % selectivity of HCAL at 100 °C under 20 bar of hydrogen pressure over the catalyst in a non-polar solvent decalin [21]. They have also compared the

catalytic activity with a commercial catalyst sample under the same reaction conditions and found it to exhibit a similar activity behavior. Kahsar et al. have reported that commercial 5 wt. % Pd/Al_2O_3 catalyst exhibits 40 % conversion with 65 % HCAL selectivity within 1 h at 50 °C under 40 bar hydrogen pressure using the polar solvent ethanol and they could improve the selectivity upto ~88 % (at 80 % conversion) by thiol coating over the catalyst [22]. Gu et al. have reported the hydrogenation activity over an ordered mesoporous carbon (OMC) containing gold and palladium nanoparticles (AuPd-OMC) under atmospheric pressure at 40 °C in isopropanol to show 97 % conversion with 88 % HCAL selectivity [32]. Palladium nanoparticle supported on a very high surface area (1181 $m^2 g^{-1}$) zeolitic imidazolate framework (Pd/ZIF) is reported to exhibit complete conversion of CAL with 90 % HCAL selectivity at 40 °C under a hydrogen pressure of 20 bar [11]. Palladium loaded over carbon nanotube and activated carbon hybrid composite is found to show a conversion of 87 % with HCAL selectivity of 82 % at 70 °C in the presence of a non polar solvent 1,4-dioxane but at a high hydrogen pressure [12]. By far the best hydrogenation activity is reported over a Pd (5 wt. %)/CNF (carbon nanofiber) catalyst exhibiting complete CAL conversion with 98 % HCAL selectivity at 80 °C under atmospheric pressure condition but requiring a reaction time of 30 h [23]. Also the carbon supported Pd-Au catalyst is reported to show CAL hydrogenation under a very mild condition (22 °C and atmospheric pressure) with 100 % CAL conversion and 65 % HCAL selectivity [37]. The activity behavior of the commercial catalyst from Aldrich is much poor (both the conversion and selectivity is less than half) and requires as high as 50 h at atmospheric pressure.

The issue of catalyst deactivation in CAL hydrogenation, if any, during cycling treatment is not so well documented in the literature [11, 12, 21, 36]. As discussed above most of these studies are performed at an elevated hydrogen pressure. Zhao et al. have reported continuous

decrease of activity over the Pd/ZIF catalyst after first run itself that is continued up to the fourth cycle of hydrogenation due to small leaching of palladium [11]. Galletti et al. have reported almost similar conversion (99-100 %) and selectivity (93.8-96.8 %) over Pd supported Al_2O_3 catalyst although they stopped the hydrogenation after the second cycle [21]. Ribeiro et al. have shown an interesting and different scenario for the Pd/CNT catalyst over which the CAL conversion under atmospheric hydrogen pressure is low, 45 % in the first cycle; which increases considerably to 99 % due to the activation of the catalyst in the second cycle and the activity remains same upto the fifth cycle of hydrogenation when HCAL selectivility remains in the range 70.7 % to 76.9 % [12]. Yu et al. have reported a magnetically separable Pd/Fe_3O_4@C catalyst that shows complete CAL conversion with very good recycling behavior (upto seven cycles), but the HCAL selectivity was 70 % [36].

From the above comparison as well as summary of activity data of **Table 3**, the CAL hydrogenation behavior under atmospheric hydrogen pressure of the present oxide based catalyst Pd2Al exhibiting good recycling characteristics and containing 4 wt. % Pd thus seems noteworthy specifically when compared with the 5 wt. % Pd/Al_2O_3 catalyst from Aldrich [23].

4. Conclusions

A Pd (2 at. %)/Al_2O_3 (Pd2Al) catalyst prepared via single step solution combustion is reported to show the best activity behavior for cinnamaldehyde hydrogenation (converts 69 % of CAL with complete HCAL selectivity) compared to other oxide supported catalysts and the analogous catalyst prepared by incipient wetness impregnation (Pd2AlIWI) under mild reaction conditions (at atmospheric pressure of hydrogen at 100 °C). In the SCS catalyst there is formation of a core-shell like structure of Pd (core)-PdO (periphery) covered with alumina layer

during hydrogenation, whereas in the IWI catalyst there is formation of a mixed Pd-PdO ensemble. This microstructural feature brings in additional stability to Pd-species in the SCS catalyst contributing to its good recycling characteristics in contrary to palladium surface species in the IWI catalyst causing continuous loss in activity in the consecutive cycles.

Acknowledgements

DD thanks CSIR and KP thanks UGC for a research fellowship. Financial support from the Science & Engineering Research Board (SERB), Government of India, by a grant (EMR/2016/001811) to AG and DST Special Grant to the Department of Chemistry of Jadavpur University in the International Year of Chemistry 2011 is gratefully acknowledged. J.L. is Serra Húnter Fellow and is grateful to ICREA Academia program and MINECO/FEDER grant ENE2015-63969-R. SC and AT acknowledges funding from Italian Ministry under FIRB project RBFR10S4OW.

References

[1] Bus E, Prins R, Bokhoven JAV (2007) Catal Commun 8:1397-1402

[2] Rase HF (2000) Handbook of Commercial Catalysts–Heterogeneous Catalysts, CRC Press LLC, Boca Raton

[3] Grolig J (2003) Ullmann's Encyclopedia of Industrial Chemistry; Wiley-VCH Weinheim, Germany

[4] Mahmoud S, Hammoudeh A, Gharaibeh S, Melsheimer J (2002) J Mol Catal A Chem 178: 161-167

[5] Gallezot P, Richard D (1998) Catal Rev Sci Eng 40:81-126

[6] Bond GC (1962) Catalysis of Metals; Academic Press London

[7] Aramendia M, Borau V, Jimenez C, Marinas J, Porras A, Urbano F (1997) J Catal 172:46-54

[8] Muller A, Bowers J (1999) WO Patent WO 99/08989 to First Chemical Corporation

[9] Sun KQ, Hong YC, Zhang GR, Xu BQ (2011) ACS Catal 1:1336-1346

[10] Müller A, Ludwig M, Arlit M, Lange R (2015) Catal Today 241:214-220

[11] Zhao Y, Liu M, Fan B, Chen Y, Lv W, Lu N, Li R (2014) Catal Commun 57:119 -123

[12] Ribeiro PHZ, Matsubara EY, Rosolen JM, Donate PM, Gunnella R (2015) J Mol Catal A Chem 410:34 -40

[13] Steffan M, Klasovsky F, Arras J, Roth C, Radnik J, Hofmeister H, Claus P (2008) Adv Synth Catal 350:1337-1348

[14] Yu W, Wang Y, Liu H, Zheng W (1996) J Mol Catal A Chem 112:105-113

[15] Yu W, Liu H, Liu M, Tao Q (1999) J Mol Catal A Chem 138:273-286

[16] Kahsar KR, Schwartz DK, Medlin JW (2015) J Mol Catal A Chem 396:188-195

[17] Shen H, Tang H, Yan H, Han W, Li Y, Ni J (2014) RSC Adv 4:30180-30185

[18] Chen X, Zhu H, Song X, Du H, Wang T, Zhao Z, Ding Y (2017) Reac Kinet Mech Catal 120:637 - 649

[19] Jhao J, Ni J, Xu J, Xu J, Cen J, Li X (2014) Catal Commun 54:72-76

[20] Malobela LJ, Heveling J, Augustyn WG, Cele LM (2014) Ind Eng Chem Res 53:13910-13919

[21] Galletti AMR, Antonetti C, Venezia AM, Giambastiani G (2010) Appl Catal A Gen 386: 124-131

[22] Kahsar KR, Johnson S, Schwartz DK, Medlin JW (2014) Top Catal 57:1505-1511

[23] Pham-Huu C, Keller N, Charbonniere LJ, Ziessel R, Ledoux MJ (2000) Chem Commun 1871-1872

[24] Nagpure AS, Gurrala L, Gogoi P, Chilukuri SV (2016) RSC Adv 6:44333 – 44340

[25] Xie R, Fan G, Ma Q, Yang L, Li F (2014) J Mater Chem A 2:7880-7889

[26] Bertolini GR, Cabello CI, Muñoz M, Casella M, Gazzoli D, Pettiti I, Ferraris G (2013) J Mol Catal A Chem 366:109-115

[27] Giang F, Cai J, Liu B, Xu Y, Liu X (2016) RSC Adv 6:75541-75551

[28] Espro C, Donato A, Galvagno S, Neri G (2016) Reac Kinet Mech Catal 118:223–233

[29] Hájek J, Kumar N, Salmi T, Murzin DY (2005) Catal Today 100:349-353

[30] Hájek J, Kumar N, Francová D, Paseka I, Mäki-Arvela P, Salmi T, Murzin DY (2004) Chem Eng Technol 27:1290-1295

[31] Pham-Huu C, Keller N, Ehret G, Charbonniere LJ, Ziessel R, Ledoux MJ (2001) J Mol Catal A Chem 170:155-163

[32] Gu H, Xu X, Chen A, Ao P, Yan X (2013) Catal Commun 41:65-69

[33] Hammoudeh A, Mahmoud S (2003) J Mol Catal A Chem 203:231-239

[34] Lashdaf M, Krause AOI, Lindblad M, Tiitta M, Venäläinen T (2003) Appl Catal A Gen 241:65-75

[35] Mehri A, Kochkar H, Daniele S, Mendez V, Berhault G, Ghorbel A (2010) Stud Surf Sci Catal 175:605-608

[36] Yu J, Yan L, Tu G, Xu C, Ye X, Zhong Y, Zhu W, Xiao, Q (2014) Catal Lett 144:2065-2070

[37] Szumełda T, Drelinkiewicz A, Kosydar R, Gurgul J (2014) Appl Catal A Gen 487:1-15

[38] Patil KC, Aruna ST, Ekambaram S (1997) Curr Opin Solid State Mater Sci 2:158–165

[39] Hegde MS, Madras G, Patil KC (2009) Acc Chem Res 42:704-712

[40] Colussi S, Gayen A, Camellone MF, Boaro M, Llorca J, Fabris S, Trovarelli A (2009) Angew Chem Int Ed 48:8481-8484

[41] Colussi S, Gayen A, Llorca J, Leitenburg C, Dolcetti G, Trovarelli A **(**2012**)** Ind Eng Chem Res 51:7510–7517

[42] Mistri R, Llorca J, Ray BC, Gayen A (2013) J Mol Catal A Chem 376:111-119

[43] Shi J, Nie R, Chen P, Hou Z (2013) Catal Commun 41:101-105

[44] Hong YC, Sun KQ, Zhang GR, Zhong RY, Xu BQ (2011) Chem Commun 47:1300-1302

[45] Lempers HEB, Sheldon RA, (1998) J Catal 175:62-69

[46] Colussi S, Gayen A, Boaro M, Llorca J, Trovarelli A, (2015) ChemCatChem 7:2222-2229

[47] Iatsunskyi I, Kempiński M, Jancelewicz M, Załęski K, Jurga S, Smyntyna V (2015) Vacuum 113:52-58